Available online at www.sciencedirect.com
ScienceDirect
Coordination Chemistry Reviews 252 (2008) 1787–1797
COORDINATION CHEMISTRY REVIEWS
www.elsevier.com/locate/ccr

Review

Cycloheptatrienyl, alkyl and aryl PCP-pincer complexes: Ligand backbone effects and metal reactivity

Wolfgang Leis [a], Hermann A. Mayer [a,*], William C. Kaska [b]

[a] *Institut für Anorganische Chemie der Universität Tübingen, Auf der Morgenstelle 18, 72076 Tübingen, Germany*
[b] *Department of Chemistry, University of California Santa Barbara, Santa Barbara, CA 93106, USA*

Received 23 September 2007; accepted 1 February 2008
Available online 12 February 2008

Contents

Abstract

Pincer complexes have developed into a class of compounds with a tremendous breadth of applications in organometallic chemistry and catalysis. In this article we have selected a few PCP-pincer ligand systems and demonstrate that small changes in the ligand backbone have a dramatic impact on the reactivity change of their metal complexes.

Keywords: PCP-pincer ligands; C–H activation; N–H activation; CO_2 activation; Hydrides

1. Introduction

Pincer ligands are terdentate ligands which coordinate in a η^3-mer fashion to a metal center (Scheme 1). The symmetric anionic bis-chelating ligands bond strongly to a wide variety of transition and non-transition metals. This bonding is achieved by the presence of at least two donor atoms and an *ipso*-carbon-metal bond, which reinforce the structure and prevent the dissociation of the metal from the ligand as well as ligand exchange processes. Early investigations have especially pointed out that the generation of two thermodynamically stable internal five-membered rings is very important [1,2]. For example the ligand backbone and the coordinating atoms can be tailored to control the bite angle, steric environment, and frontier orbitals [3,4]. Furthermore, the meridional arrangement of the pincer ligands force all participating ligands into *cis*-positions. Together these factors translate into materials with exceptional thermal stability and still high reactivity [5–8]. Since their first inceptions [2,9–12] the diversity of pincer ligand systems has increased dramatically which also has widened the application in many areas like organometallic chemistry, reaction mechanisms, catalysis and design of new materials. Thus, pincer ligand systems have left the state of curiosity and are nowadays integral parts of many concepts in chemistry [4,5,13–18].

The most popular pincer ligands remain those with aryl backbones (Scheme 1, **I**). The rigid phenyl ring and the strong sp^2-carbon-metal bond makes them ideal candidates for studying synthetic, catalytic and mechanistic properties of the complexes. Pincer ligand complexes with an alkane backbone **II** have been less attractive. The high flexibility of the alkane rings as well as the higher electron-donating ability of the *ipso*–sp^3-carbon atom in the corresponding metal complexes

* Corresponding author. Tel.: +49 70 71 29 76229; fax: +49 70 71 29 2436.
E-mail address: hermann.mayer@uni-tuebingen.de (H.A. Mayer).

0010-8545/$ – see front matter © 2008 Elsevier B.V. All rights reserved.
doi:10.1016/j.ccr.2008.02.002

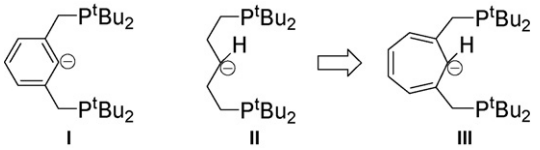

Scheme 1.

increase their reactivity which makes them more difficult to manipulate.

A novel way to expand the pincer ligand backbone is to incorporate the cycloheptatriene moiety into the ligand backbone (Scheme 1, **III**). Previous work has demonstrated that this moiety can be an interesting and vital part of a pincer ligand system [19–21]. The particular feature of the cycloheptatrienyl pincer complexes is their unsaturated but non-aromatic ligand backbone. This makes the cycloheptatriene moiety an intermediate between the phenyl- and alkane-based pincer ligands.

The differences in chemical behavior of the aryl, alkyl and cycloheptatriene pincer complexes can be rationalized by comparing the resonance structures displayed in Scheme 2. The selected examples display metal-carbon bond polarities which are favored by the respective ligand backbone. For instance, if X = H the resonances structures $\mathbf{I}_A$ and $\mathbf{I}_C$ contribute modestly to the overall bonding situation in the aryl system. Modification of the backbone with electron withdrawing or donating substituents X can influence the contribution of $\mathbf{I}_A$ and $\mathbf{I}_C$. As an example the metallaquinone $[O{=}C_6H_2\text{-}(CH_2P^tBu_2)_2]Ru(CO)_2$ [14,22] can be derived from $\mathbf{I}_C$. Spectroscopic evidence supports the alkylidene structure $\mathbf{II}_A$ in the case of the alkyl complex. Furthermore, it is expected that the positively charged character of the aromatic 6π-electron system of the cycloheptatrienyl ring will impose a reversed polarity. Thus, resonance structure $\mathbf{III}_C$ (Scheme 2) will gain importance.

2. Aryl as the ligand backbone

The sensitivity of reactivity towards substituents in the *para* position has been demonstrated by the dehydrogenation/hydrogenation equilibrium displayed in Scheme 3. Substituent X is able to shift the equilibrium towards **2** or **1**. The electron-donating methoxy group in compound **1b** leads to a stabilization of the resonance structure $\mathbf{I}_C$ which increases the electron density at the metal and facilitates the intramolecular oxidative addition of a *tert*-butyl C–H bond. This allows the isolation and full characterization of **2b** [23]. In the case of the unsubstituted complex **1a** (X = H) the dehydrogenation to **2a** has never been observed. On the other hand storage of the nitro compound **1d** for a few months leads to a complete conversion to **2d**, while **2c** is quantitatively formed from **1c** in solution within 5 days [24]. These observations agree with conclusions drawn from theoretical investigations that the π-donating/withdrawing abilities of the substituents in the *para* position dominate the reactivity [25,26]. The substituents MeO, OH, NO_2 and NHR in the complexes **1b–e** possess these characteristics only in those compounds that support the resonance structures $\mathbf{I}_A$ and $\mathbf{I}_C$ which contribute to the overall stability. The σ-donating capability of the MeO group in **1b** is then responsible for the importance of $\mathbf{I}_C$ which increases the electron density at the metal for the second C–H activation process. Thus, **2b** is obtained by two consecutive intramolecular C–H bond activations. Details about the sp^3-C–H bond activation which is accompanied by a dehydrogenation are still unclear. Quantum chemical calculations show that **2a**,**b** are thermodynamically less stable than **1a**,**b**. Furthermore, electrochemical studies established an equilibrium between **1a**,**b** and **2a**,**b** + H_2. The isolation of **2b** is only realized if H_2 is expelled from the reaction mixture.

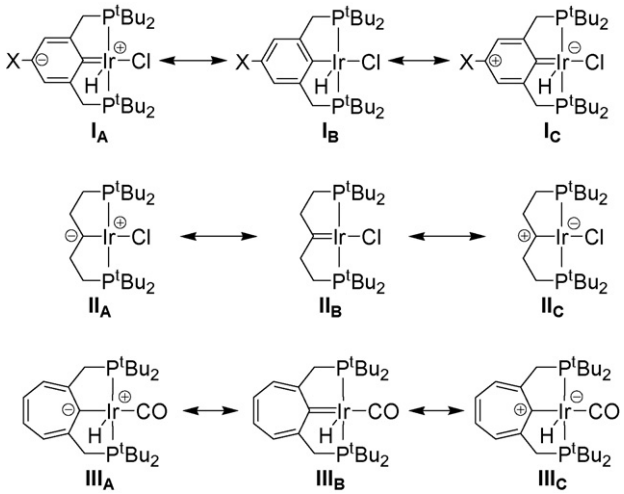

Scheme 2.

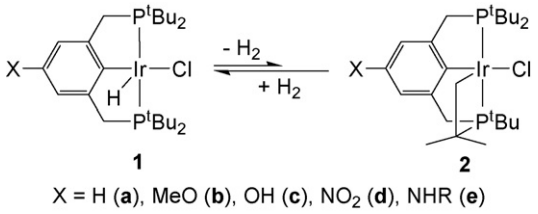

Scheme 3.

A more detailed electrochemical investigation revealed that the electrode reaction mechanisms for both **1a**,**b** involve a joint feature called a square scheme with a coupled ECE reaction sequence (follow-up reactions) (Scheme 4) [27]. The electron transfer reactions are linked by two chemical equilibria which have been shown to be homogeneous hydrogenation/dehydrogenation steps. Interestingly, the one-electron transfer oxidation of both **1a**,**b** reverses the stability of the two pincer complexes related to C–H activation. While the hydridochloride form is favored in the Ir(III) oxidation state, after oxidation the doubly cyclometalated species prevails. It is important to note that for both compounds the intramolecular C–H activation step is promoted by one-electron oxidation. The same effect has been reported previously for $IrMe_2(\eta^5\text{-}C_5Me_5)PR_3$ (R = Me, Ph). Here upon oxidation of the iridium(III) complex to the Ir(IV) cation $[IrMe_2(\eta^5\text{-}C_5Me_5)PR_3]^+$ the rate of the C–H activation has been dramatically increased [28–30].

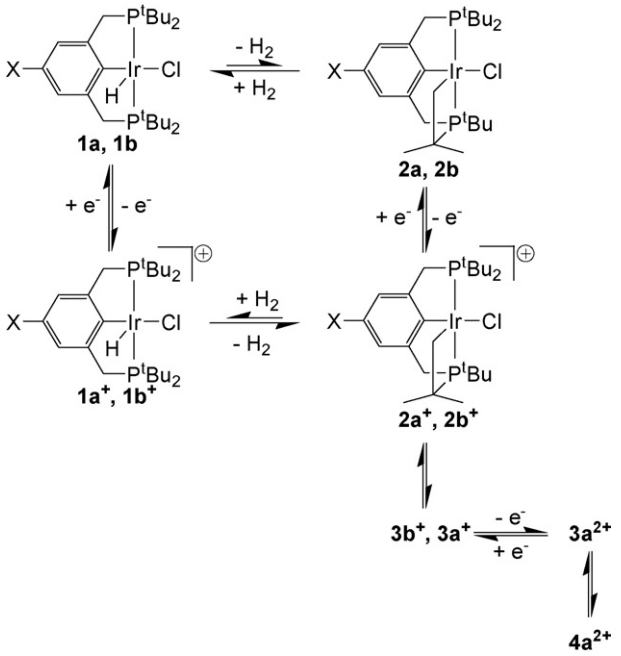

Scheme 4.

Significant differences between the electrochemical behavior of **1a** and **1b** involve a shift of the peak potentials to more positive values in **1a** compared to **1b**. This has been explained as a result of the decrease of the electron density at the iridium center in the unsubstituted complex **1a** as compared to the methoxy compound **1b**. Therefore, the release of an electron in the oxidation process becomes more difficult. Interestingly, the chemical equilibrium in the oxidized part of the square scheme is more facile for **1a** compared to **1b**.

In the case of **1b**, the one-electron oxidation product of the square scheme reacts only slowly to electrochemically inactive $\mathbf{3b}^+$. This is in contrast to **1a** where the product $\mathbf{2a}^+$ quickly undergoes further transformations (Scheme 4). The follow-up products $\mathbf{3b}^+$, $\mathbf{3a}^+$, $\mathbf{3a}^{2+}$ and $\mathbf{4a}^{2+}$ have not been characterized in detail, however, their mechanistic importance is strongly indicated by experimental and simulated data [27].

From the shape and the high intensity of the oxidation peak of **1a** it has been interpreted that a further electron transfer process contributes to the initial one-electron oxidation with the possible formation of an Ir(V) species. Overall, the kinetic and thermodynamic parameters derived from a comparison of cyclic voltammetric experiments and computer simulations confirm the assumption that the intramolecular C–H activation is promoted by one-electron oxidation of **1a** or **1b**. Up to now only **2b** could be isolated and characterized which might be due to the more facile oxidation of **1b** compared to **1a**.

Thus, in contrast to **1b** the hydridochloro rhodium complex **5** has to be reduced to a highly reactive $14e^-$ species to oxidatively add C–H bonds (Scheme 5) [31]. As deduced from spectroscopic and experimental data intermolecular oxidative addition of solvent molecules as well as the intramolecular addition of a *tert*-butyl C–H bond takes place. This has been the first time that it has been mentioned that the *tert*-butyl groups of pincer

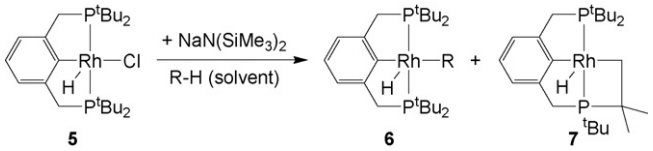

Scheme 5.

complexes are able to compete with intermolecular C–H activation. Further *tert*-butyl group activation in iridium and ruthenium pincer complexes have been reported recently [16,32].

3. Alkyl as the ligand backbone

The more σ-electron-donating character of sp^3-carbon atoms compared to sp^2-carbons increases the electron density at the metal center significantly. This might be one reason for the stability of the carbene complex **9**, that has been prepared first by thermal decomposition of **8** in around 5% yield [33] or later in yields around 60% by continuous photolysis and removal of H_2 (Scheme 6) [34].

The hydride–borane complex **12** is the product of the substitution of the chloride by a hydride ligand followed by the coordination of the leaving BH_3 molecule when **9** is treated with $NaBH_4$. This behavior of **9** in presence of the nucleophilic boronhydride anion supports the importance of the alkylidene resonance structure $\mathbf{II}_A$ (Scheme 2). In **12** the *trans* orientation of the strong field carbene ligand is evaded and the μ^2-bridging hydride ligands strongly reduce the donated electron density to the iridium center.

Treatment of **9** with carbon monoxide leads to the formation of the adduct compound **10**, accompanied by complex **11** which is the product of α,β-hydride shift. Carbon monoxide as a strong σ-donor as well as an efficient π-acceptor ligand seems to destabilize the carbene metal bond and therefore induces β-H-elimination. Similar rearrangements have been reported for rhodium [35,36], ruthenium and osmium [37,38] complexes with alkyl-based pincer ligands.

The Ru(II) carbene complex **15** for example coexists in an equilibrium with the olefin complex **13** (Scheme 7). From DFT calculations [39] it is concluded, that these 1,3-bisaminopropane-based pincer complexes show a distinct competition between α-H- and β-H-elimination so that all accessible isomers are observed in the equilibrium. Thermodynamically the Ru(II) olefin complex **13** is the most stable form,

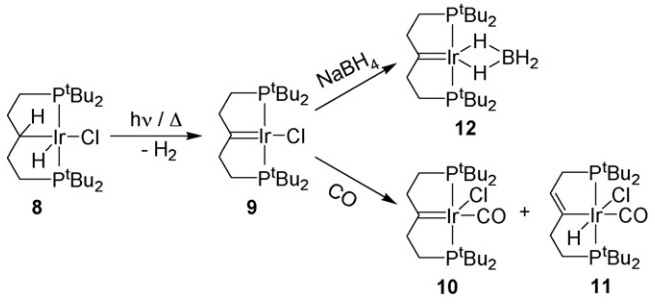

Scheme 6.

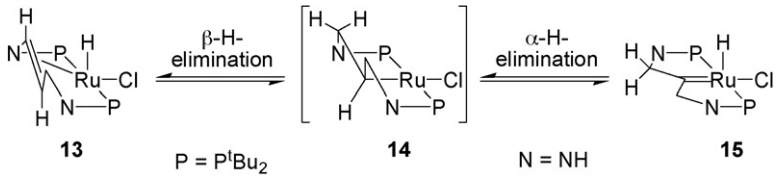

Scheme 7.

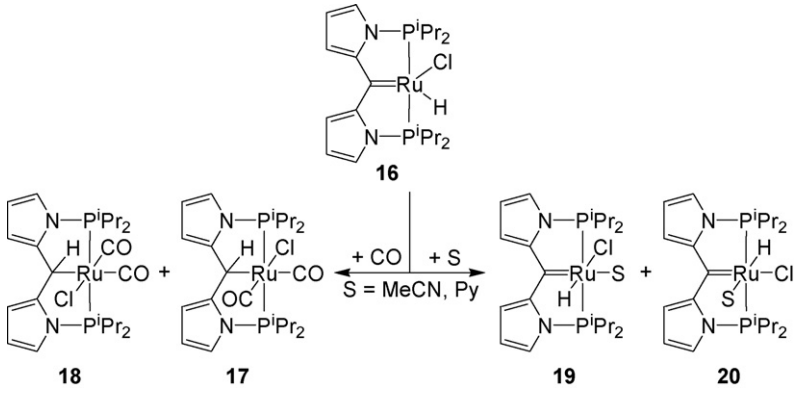

Scheme 8.

although the carbene compound **15** is only 2.9 kcal/mol higher in energy. It should be emphasized that mechanistically the spin change from a singlet ground state in **13** or **15** to a triplet ground state for the 14e$^-$ alkyl intermediate **14** seems to be involved.

In order to obtain π-acceptor properties of the carbene atom, a PCP-pincer backbone without β-H-atoms has been developed, that is not able to undergo carbene–olefin isomerization (Scheme 8) [40].

The Ru(II) complex **16** (Scheme 8) is obtained in very good yield by treatment of the dipyromethane PCP ligand with [(*p*-cymene)$RuCl_2]_2$ and triethylamine at 100 °C in toluene. The products of the reaction of **16** with pyridine or acetonitrile are proposed to be the adduct compounds **19** and **20** which are detected at low temperatures. At room temperature *just an overlayed* structure is observed. Again the *trans* orientation of hydride and carbene ligands is avoided, because both are strong field ligands. Treatment of **16** with CO leads to a mixture of the two isomers **17** and **18** where two CO molecules are coordinated to the ruthenium center. The disappearance of the hydride signal in the ^{1}H NMR spectrum is explained by a 1,2-hydride shift to the carbene atom. Compounds **17** and **18** are designated as the *syn*- and the *anti*-isomer with respect to the H–C–Ru–Cl unit. Similar to the reaction displayed in Scheme 6 the coordination of CO *trans* to the carbene carbon atom is avoided by a 1,2-hydride shift (α-elimination) to the carbene atom (analog Scheme 7) and the formation of a carbon-metal σ-bond *trans* to CO.

Recently the alkyl pincer complex **22** has been shown to oxidatively add ammonia to form the hydridoamide complex **23** (Scheme 9) [41,42]. This is remarkable as ammonia prefers to coordinate via the lone pair. To obtain an efficient precursor for the assumed highly reactive 14e$^-$ Ir(I) intermediate, the hydridochloro complex **8** is treated with superhydride ($Li[HBEt_3]$) in a hydrogen atmosphere to obtain the tetrahydrido compound **21** that subsequently is transformed to the propene complex **22**.

Treatment of **22** with ammonia at room temperature results within 5 min in 90% yield in the hydridoamide **23**. Independently **23** has been isolated by treatment of **8** with ammonia in presence of the strong base $K[N(SiMe_3)_2]$. Mechanistic considerations of the N–H activation based on thermodynamic and kinetic studies as well as labeling experiments ruled out pathways *via* hydrido carbene or double cyclometalated intermediates. Also an associative pathway can be excluded. Most likely the reaction proceeds *via* the dissociation of propene followed by the N–H oxidative addition of ammonia [41]. In case of the aryl-based pincer complexes the analogous hydridoamide **25** is accessible in a two-step synthesis (Scheme 10). Treatment of the hydridochloro complex (**I**$_B$ with X = H) with ammonia leads to the classic Ir(III) ammonia complex **24** which could also be converted into **25** by addition of $K[N(SiMe_3)_2]$ to the reaction mixture at −78 °C.

Interestingly the aryl pincer amide **25** is more labile than the alkyl pincer complex **23** and reductively eliminates ammonia

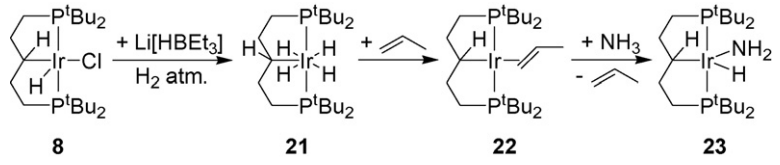

Scheme 9.

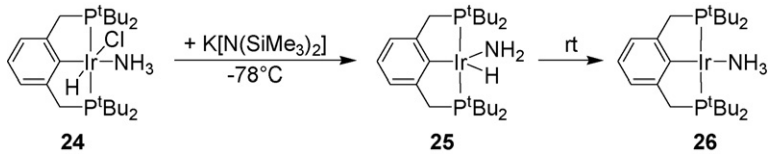

Scheme 10.

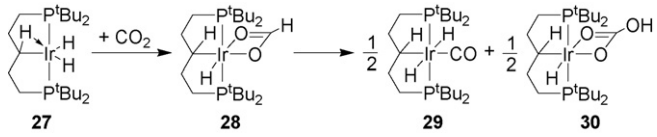

Scheme 11.

rapidly at temperatures above −10 °C to form the Ir(I) ammonia complex **26**. The aliphatic backbone induces a higher electron density on the metal center than the aromatic backbone which forces the oxidative addition of ammonia in the case of **23**. This is plausible because the process of oxidative addition is associated with electron donation from the metal to the substrate and hence reduces the electron density at the metal. *Vice versa* the reductive elimination increases the electron density at the metal and is therefore preferred in the aryl pincer complex [41,42].

Further examples for small molecule activation with PCP-pincer complexes are the formation of formate complexes from CO_2 (Scheme 11). The alkyl iridium dihydride pincer complex **27** rapidly generates the formate complex **28** in the presence of carbon dioxide [43]. Over a period of some weeks **28** undergoes a disproportionation to the *trans*-dihydride species **29** accompanied by the crystallization of the bicarbonate complex **30** from the reaction mixture.

Complex **27** is accessible from the tetrahydride **21** by careful sublimation. The penta-coordinated Ir(III) dihydride **27** is described with an agostic interaction from the methyne C–H bond. This could be explained by the donation of electron density from the electron-rich metal into the σ*-orbital of the C–H bond.

The very similar reaction of the rhodium analog η^2-dihydrogen complex **31** with carbon dioxide forms the rhodium formate compound **32** (Scheme 12) [35]. The same product is obtained by treating the CO_2 adduct **33** with hydrogen. It is assumed that the latter reaction proceeds *via* the dihydrogen complex **31** as intermediate.

In case of the aryl-based rhodium PCP-pincer complex the formate **35** is characterized in the reaction mixture by ^{13}C NMR and IR spectroscopy [44]. It is as well available from the dihydrogen complex **34** by treatment with carbon dioxide. Over a period of some hours **35** loses CO. If the reaction is allowed to continue for 1 week or more, the Rh(I) carbonyl complex **37**

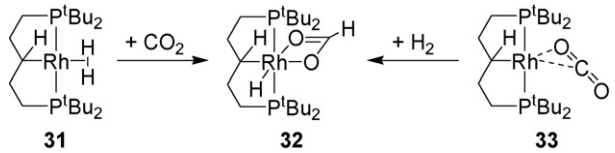

Scheme 12.

is obtained. Independently **37** can be prepared by treating the isolated and redissolved compound **36** with CO.

In order to get a deeper understanding of the different behavior of the rhodium PCP-pincer complexes depicted in Schemes 12 and 13 a combined experimental and DFT investigation has been performed recently [45]. To examine the possible reaction pathways the calculations are performed with PCP complexes which contain hydrogen atoms instead of *tert*-butyl groups at the phosphorus atoms. The first reaction step is supposed to be the formation of the exergonic dihydrogen coordinated rhodium center which weakly binds to η^1-CO_2. Subsequently the CO_2 moves to the η^1-*O*CO coordination which is an endergonic process. The four-membered transition state of the hydride shift to the CO_2 carbon atom forms the η^1-OOCH complex which rearranges fast to the strongly exergonic hydrido formate complex **32** or **35** with the η^2-OOCH unit. It should be noted that the alkane-based formate complex **32** is thermodynamically more stable than the phenyl-based **35**. In case of reductive elimination of formic acid the five-membered transition state is thermodynamically and kinetically favored for the aryl-based rhodium pincer complex **35**, while the alkane-based pincer complex **32** requires a higher activation barrier and leads to less stable products. The observation of **36** and **37** might be realized in the ease of formic acid elimination from complex **35**.

4. Cycloheptatrienyl as the ligand backbone

Cycloheptatrienyl organometallic compounds with their various modes of bonding in the form of η^1-carbene, η^2-allene and η^7-tropylium complexes were studied many years ago [46–50]. The seven-membered monocyclic C_7H_6 ring has two isomers, the cycloheptatrienylidene (CHD) and the cyclohepta-1,2,4,6-tetraene (CHTE) on the C_7H_6 energy surface. Although the allene (CHTE) is the most stable species, the carbene (CHD) presumably is the lowest energy transition state on the isomerization pathway between enantiomeric allenes [51,52]. Different transition metal complexes are able to respond to the C_7H_6 isomers and stabilize their characteristic structural features *via* different bonding modes. Thus, early transition metals are in favor of the carbene (cycloheptatrienylidene) structure [53]. This has been explained by the aromaticity of the tropylium resonance form and the low-lying vacant orbitals on the metal which are important for σ-bond formation [48]. Late transition metals show a more differentiated behavior. While platinum(0) favors the allene structure a carbene could be established for a d^8 Pt(II) complex due to the strong interactions between the cycloheptatrienylidene HOMO and the metal LUMO [48].

The introduction of di-*tert*-butylmethylenephosphane moieties in 1,6 position of 1,3,5-cycloheptatriene generates a

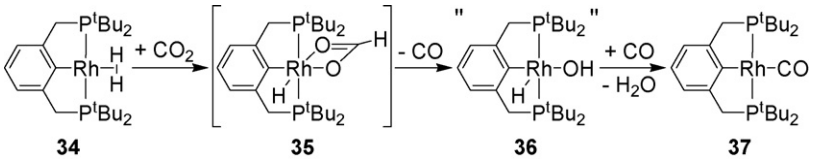

Scheme 13.

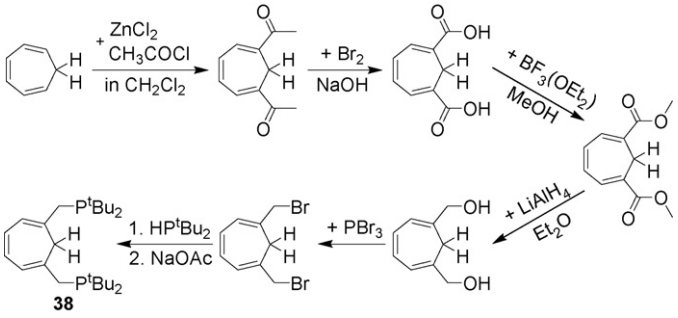

Scheme 14.

PCP-pincer ligand which locates the metal next to the CH_2-group of the cycloheptatriene ring. The oxidative addition of one C–H bond forms a PCP-pincer complex with a sp^3-C–H metal bond which is similar to the alkyl PCP complex **8** in Scheme 6.

In Scheme 14 the synthetic pathway to the cycloheptatriene (CHT) PCP-pincer ligand **38** is depicted as described [19]. A zinc dichloride assisted acylation of cycloheptatriene is followed by oxidation with bromine and an esterification to obtain the dimethylester. Reduction to the diol, bromination and finally introduction of the phosphine completes the ligand synthesis. If reduction of the diester with $LiAlD_4$ is employed the methylene protons of both phosphine arms in **38** are selectively replaced by deuterium [54].

Preparation of pincer metal complexes from **38** with different metal precursors turned out to be more difficult than in the cases of the analogous phenyl or alkyl pincer ligands. Indeed, **39** is generated from **38** with tricarbonyl iridium chloride in a clean reaction (Scheme 15) whereas the procedures with iridium trichloride hydrate or with the cyclooctene or cyclooctadiene complexes of iridium led to complicated reaction mixtures where no CH_2 carbon metalation could be observed. The main difference at the metal site between the alkyl pincer complex **8** and the cycloheptatrienyl pincer complex **39** is the carbonyl ligand which gives rise to the coordinatively as well as electronically saturated compound **39** in contrast to the five coordinated $16e^-$ complex **8**. This provides the carbonyl complex **39** with a higher stability. As the carbonyl in **39** is located *trans* to the metal-carbon atom the hydride and the chloride ligands are forced into a mutual *trans* orientation. The C–H group in the CHT backbone in **39** is strongly bent out of the plane which encompasses the three double bonds. Consequently the residual hydrogen atom at the metal bound sp^3-carbon and the chloride ligand are *syn*-periplanar at the iridium center. In order to transform **39** into a more reactive species several approaches to remove CO has been attempted, however, without success [19]. Therefore, the cycloheptatrienyl PCP complex **39** has been treated with different electrophiles as well as nucleophiles displaying rather unusual reactivities [19–21]. Surprisingly, when trimethylsilytriflate was applied to displace the chlorine atom from the metal in **39** complex **40′** (with triflate as counterion) is formed (Scheme 15).

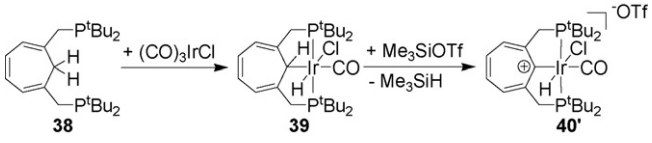

Scheme 15.

This is explained by the abstraction of a hydride from the *ipso*-carbon atom which generates an aromatic tropylium cation in the ligand backbone while the chlorine at the metal remains untouched. The crystal structure analysis by XRD reveals a planar CHT backbone which is twisted from the equatorial plane containing the two phosphorus, the *ipso*-carbon and the carbonyl by about 10–20°.

The increased aromaticity of the backbone in the cation **40** is confirmed by ^1H and ^{13}C NMR spectroscopy as well as by the η^7-coordination of a tricarbonyl molybdenum fragment (Scheme 16) [20]. Already at low temperatures the *para*-xylene is replaced from (η^6-*para*-xylene)tricarbonyl molybdenum by the cationic PCP complex **40** to generate the heterobimetallic molybdenum iridium compound **41**. Interestingly, the complex **41** represents a rare example in which one sp^2-carbon atom of the cyclic ring coordinates to two different metals *via* two binding modes. The η^1:η^7-coordination is achieved *via* an iridium carbon σ-bond and *via* a delocalized π-bond between the cycloheptatrienyl ring and the molybdenum fragment. A similar bonding situation has been reported for the $[(OC)_2CpFe(\mu\text{-}\eta^1\text{:}\eta^7\text{-}C_7H_6)Cr(CO_3)]^+$ cation [49,50] and metallocene pincer complexes [55–58].

Surprisingly the treatment of **39** with $Li[HBEt_3]$ leads to the alkylated compound **42** and a *trans* dihydride complex **43** (Scheme 17) [19]. The unexpected ethyl complex **42** is the major product. Obviously, $Li[HBEt_3]$ in this reaction is transferring an ethyl group which contrasts the general use of boronhydrides as hydride transfer agents [59]. The isolation of **43** is unexpected as well because *trans* dihydride complexes are rare

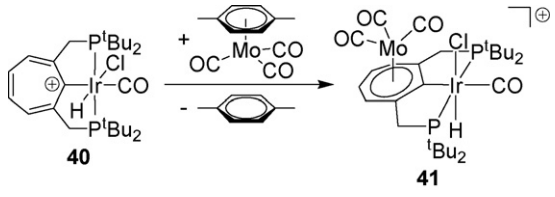

Scheme 16.

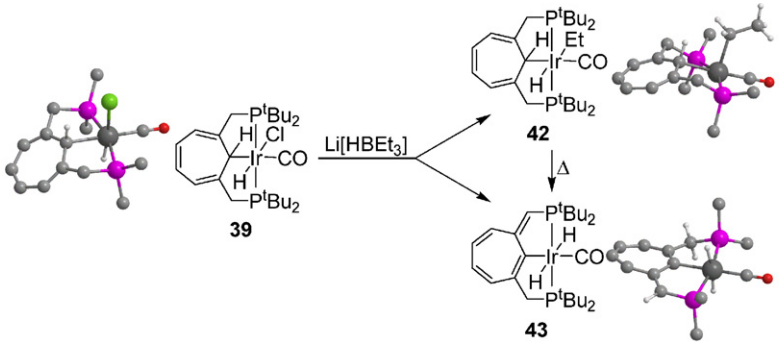

The depicted ball-stick structures are from DFT B3LYP/LACVP* geometry optimizations.
For clarity most of the hydrogen atoms and methyl groups have been omitted.

Scheme 17.

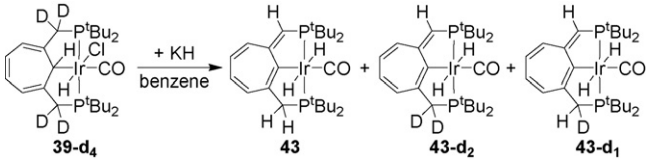

Scheme 18.

due to the strong *trans* effect of the hydride ligand. The formation of **43** is initiated by Li[HBEt$_3$] which is acting as a strong base. Thermal decomposition of independently synthesized **42** leads to the dihydride **43** too. A β-elimination of ethylene is unlikely because of the absence of a vacant coordination site at the metal. But the calculated ball–stick structure of **42** reveals an auspicious situation for a *syn*-periplanar β-elimination of ethane forming a carbene intermediate which then rearranges to the dihydride **43** [60]. Energetically the formal loss of HCl from **39** to **43** is an endergonic process with 28.6 kcal/mol. Compound **42** is 16.8 kcal/mol and 27.5 kcal/mol higher in energy than the anticipated carbene and the dihydride **43**, respectively (see Scheme 23). This makes the transformation from **42** to **43** a thermodynamically favored process, while the elevated temperatures point to a high activation barrier of the reaction.

The treatment of the deuterated pincer complex **39**-**d**$_4$ with potassium hydride in benzene leads to a mixture of the different *trans* dihydride isotopomers **43**, **43**-**d**$_2$ and **43**-**d**$_1$ (Scheme 18) [54]. This observation suggests an initial deprotonation of the deuterated methylene bridges with subsequent proton shifts, chloride elimination and redistribution of the π-system in the backbone.

Further investigations about the contribution of direct H/D exchange of the CD_2-moiety with KH or the exchange of iridium bound deuterium with CH bonds of the solvent are still in progress.

In Scheme 19 the behavior of the CHT PCP-pincer complex **39** with the bases 1,8-diazabicyclo[5,4,0]undec-7-ene (DBU) and lithium 2,2,6,6-tetramethylpiperidide (LiTMP) under different conditions is illustrated [21].

Over a reaction time of 4–5 days in refluxing THF the non-coordinating relatively weak base DBU produces as major product the dihydride Ir(III) complex **43** and, induced by column chromatography, the Ir(I) complex **44** which has lost a further equivalent of H_2. The reaction of the more basic and bulkier base LiTMP under comparable conditions has been monitored by ^{31}P NMR spectroscopy. Within the first 5 days an increase of the concentration of **43** up to 70% has been detected. The following decrease in concentration of the dihydride **43** is accompanied by increasing amounts of **44** [60]. Therefore, it is concluded that **43** and **44** do not form simultaneously. Complex **43** is formed initially and subsequently loses dihydrogen to generate **44**. If the reaction with DBU is performed at room temperature and monitored over a period of time of 40 days a rearrangement to the Ir(I) complex **45** is observed (Scheme 19). Consecutive

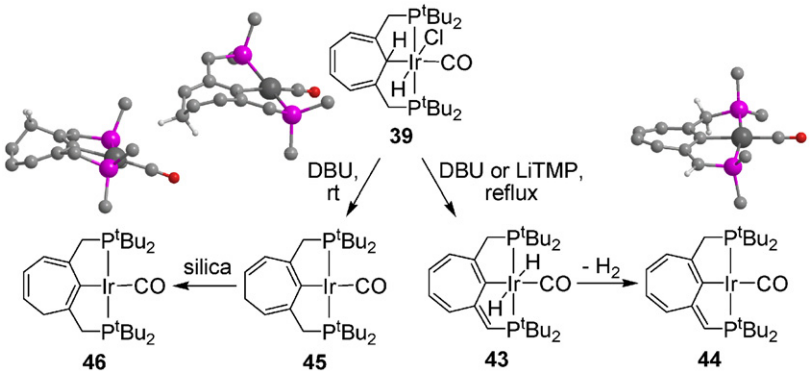

Scheme 19.

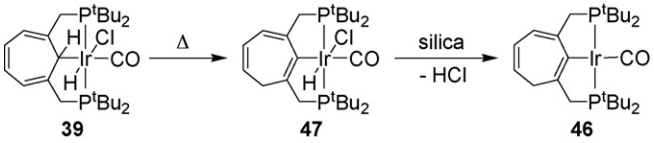

Scheme 20.

chromatographic separations of the crude reaction mixture lead to growing concentrations of **46**.

From DFT calculations [60] (Scheme 23) it can be estimated that the dehydrogenation which leads to complex **44** is an endergonic reaction step with 9.1 kcal/mol. Compound **45** is 10.5 kcal/mol more stable than the dihydride **43** and therefore destabilized by 18.1 kcal/mol relative to **39**. The formation of **43** is more endergonic than the alternative creation of **45**. Complex **46** is stabilized by 15.9 kcal/mol and 5.4 kcal/mol compared with **43** and **45**, respectively.

Complex **46** is accessible by heating the neutral hydridochloro complex **39** without a base in THF and subsequent column chromatography (Scheme 20). The structure of intermediate **47** has been elucidated by NMR spectroscopy from the reaction mixture and confirmed by the observation of **46**. Calculations predict an exergonic reaction from **39** to **47** with 7.6 kcal/mol. The following silica assisted reductive elimination of HCl from the Ir(III) complex **47** forms the product **46** which is destabilized by 20.3 kcal/mol compared to **47**.

Also complex **44** can be synthesized *via* an alternative route. Treatment of the cationic complex **40** with 1 equiv. of aqueous sodium hydroxide deprotonates one of the methylene bridges which is accompanied by the redistribution of the π-system generating the Ir(III) complex **48** (Scheme 21).

A further equivalent of sodium hydroxide induces the reductive elimination of HCl from the iridium atom to form **44**. The reverse reaction from **44** is achieved by the application of stoichiometric amounts of aqueous hydrochloric acid.

4.1. Mechanistic considerations

It is assumed that the formation of **49** and **50** is preceded by a deprotonation step in **39**. Scheme 22 depicts three positions in complex **39** where a base can possibly attack to remove a proton:

(A) The base abstracts the proton from the *ipso*-carbon atom initiating a *syn*-periplanar β-elimination of HCl which results in the Ir(I) carbene structure **49**. It is supposed that **49** is a key intermediate in the reaction of **39** with strong bases (Scheme 19, see also below).

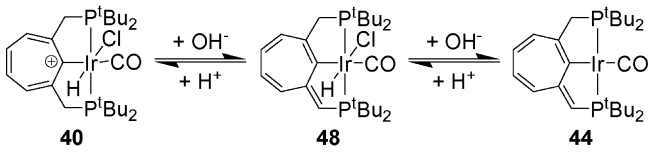

counterions have been omitted

Scheme 21.

DFT calculations (B3LYP/LACVP*) suggest the energetic availability of the carbene structure **49** being approximately 39.3 kcal/mol and 10.7 kcal/mol higher in energy than complex **39** and the dihydride **43**, respectively (Scheme 23). The formation of **43** can be understood as a decomposition of the carbene **49** by a 1,4-proton shift (γ-elimination) from one of the methylene protons to the iridium center which is accompanied by the rearrangement of the backbone. This rearrangement is driven by the stability of the metal sp^2-carbon bond.

(B) The abstraction of H$^+$ from the acidic bridging methylene groups, rearrangement and reprotonation of the resulting carbanion are possible subsequent reaction steps, which can explain the observed backbone rearrangements, e.g. in compound **47**.

(C) A base catalyzed reductive elimination of HCl from the iridium center forms the Ir(I) complex **50** which is an isomer of the carbene **49**. The accessibility of an aromatic tropylium system in **50** by removing a hydride from the *ipso*-carbon atom supports a 1,2-proton shift (α-elimination) to the metal which would form the carbene complex **49**. A similar rearrangement is described in the case of the alkyl ruthenium PCP-pincer complexes **14** and **15** in Scheme 7. Indeed the results from DFT calculations predict **50** as a thermodynamically stable structure which is 18.5 kcal/mol more stable than the carbene **49** and remains 7.8 kcal/mol below the dihydride **43** (Scheme 23).

So far it is not completely clear, whether, the deprotonation pathway depends on the base or the conditions applied [21]. But it seems to be very intuitive, that the proton abstraction from the methylene bridges (way B) should be the kinetically favored process.

The explanation of the formation of the isomeric complex **45** from the carbene **49** requires a 1,5-hydrogen shift from the metal to the backbone. In case of an unimolecular reaction this 1,5-hydrogen shift seems to be unlikely because of the inappropriate geometric situation in such a transition state. A more convenient mechanistic proposal uses the deprotonation of the methylene bridges (way B, Scheme 22) and the assumption of an equilibrium between the relatively strong conjugated acid of DBU and the resonance stabilized carbanion of the complex.

Mechanistically most of the backbone rearrangements as well as the different metal coordination states are explained in the proposed reaction mechanisms in Scheme 24. The main aspect of the reaction of **39** with bases (B) is the deprotonation of the bridging methylene groups. The depicted resonance structures of the carbanion **51–53** are the reason for the increased acidity of the methylene protons and explain the ease of backbone rearrangements compared to alkyl pincer complexes. The isomeric Ir(I) complexes **45** and **46** (Scheme 19) can be obtained by reprotonating the resonance forms **52** and **53**, respectively by the conjugated acid (HB). Forms **56** and **47** are available by 1,3-proton shifts from the *ipso*-carbon atom to the bridging methyne group. From Scheme 23 it is evident that the stability patterns of the Ir(I) species **45** and **46** are reflected in the more stable Ir(III) species **56** and **47**, respectively. Furthermore it should be noted,

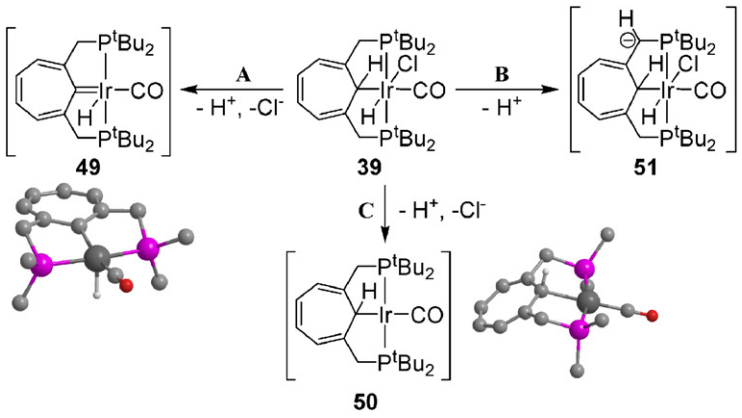

Scheme 22.

that also interconversions between **56** and **47** or **45** and **46** *via* 1,3-hydrogen shifts are conceivable. It is quite interesting that in the case of the experimentally confirmed Ir(III) intermediate **47** the free enthalpy of formation relative to **39** turns out to be exergonic in comparison to **56** where the reaction proceeds nearly thermoneutral (Scheme 23). The free formation enthalpy for the reductive elimination of HCl forming the Ir(I) complexes **46** and **45** is with around 20 kcal/mol and 18 kcal/mol comparatively endergonic.

A further stabilization pathway for the carbanion **51** is the 1,3-proton shift (allyl shift) from the *ipso* carbon to the bridging methyne carbanion accompanied by the elimination of a chloride ion from the iridium producing carbene **49**. The 1,2-hydride shift generating complex **50** from the metal to the *ipso* carbon is, as mentioned, before thermodynamically not favored. However, both structures are possible precursors for the dihydride complex **43** whereas the formation from the carbene **49** can be understood as a 1,5-proton shift (γ-elimination) from the methylene bridge to the metal.

Starting from **50** either the first step is a 1,2-hydride shift forming the carbene back or the first step is the γ-elimination followed by a 1,2-hydride shift (Scheme 24). These considerations make the formation of the dihydride **43** *via* the carbene **49** more likely than *via* the intermediate **50**. A further argument for the carbene as reactive intermediate is that formation of **43** and **44** is exergonic starting from the carbene **49**. Mechanistically the hydride transfer from the metal to one of the methylene protons in **49** describes the loss of H_2 and the rearrangement to **44**.

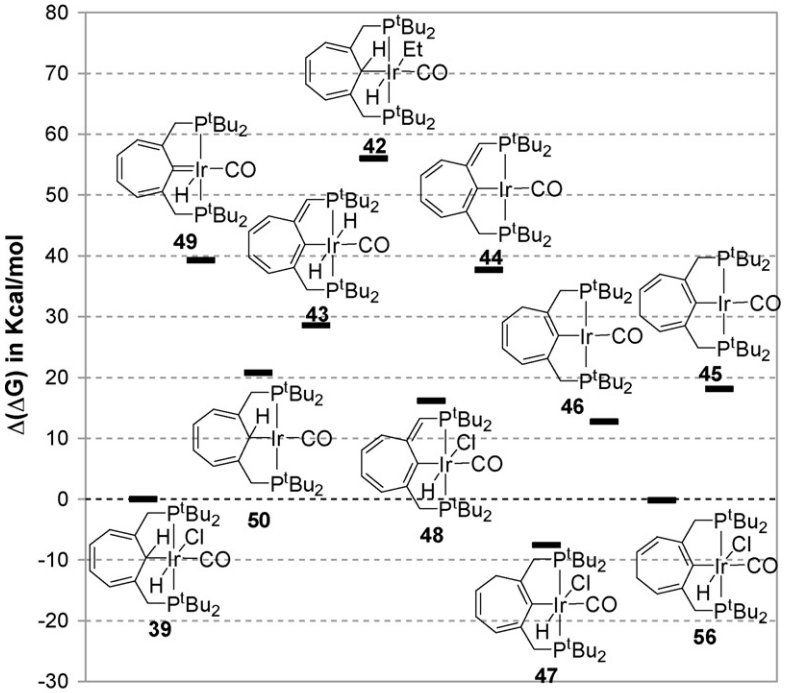

Comprehensive energy scheme of all CHT Pincer complexes. The DFT (B3LYP/LACVP*) energies are relative to complex **39**. [60]

Scheme 23.

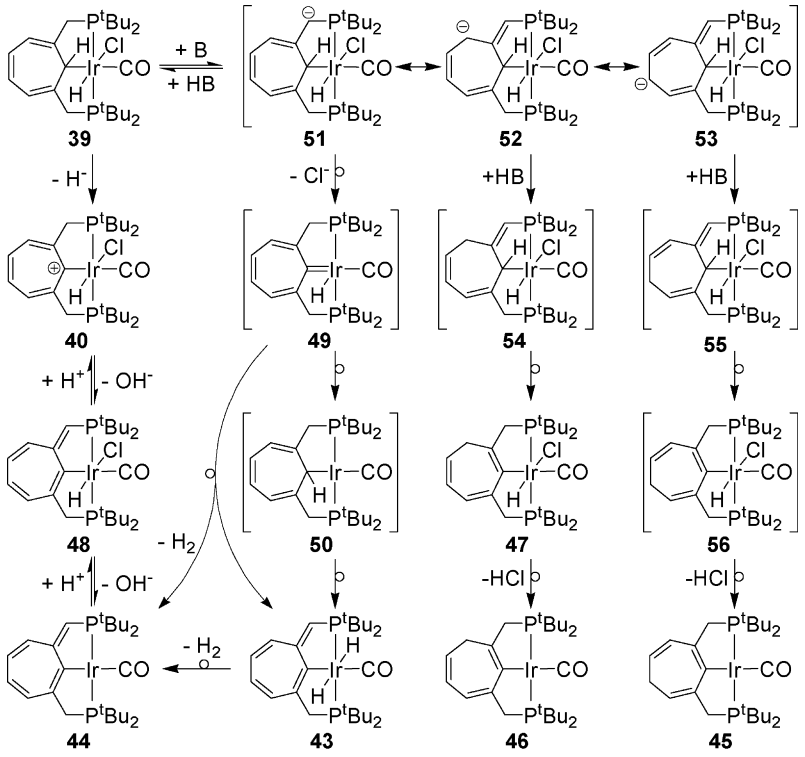

Proposed mechanistic considerations. B stands for different bases, BH are their conjugated acids.

Scheme 24.

The different behavior of **39** towards the different bases DBU, LiTMP, KH and NaOH can be explained by the steric hindrance and the basicity of KH and LiTMP. The strong bases do not allow reprotonation of the resonance forms **51**–**53** and force the carbanion to eliminate a chloride ion, which forms the carbene **49**. The bulkiness of LiTMP slows down the reaction rates of the deprotonation. The application of the significantly weaker base DBU at ambient temperature leads to the products **45** and **46** which are thermodynamically more stable and probably kinetically favored compared to **43** and **44**, respectively. At higher temperatures the rate constant for the carbene pathway seems to rise and consequently the products **43** and **44** are observed additionally.

After elimination of a hydride ion **39** generates the cationic compound **40**. It is very easy to deprotonate the cationic complex **40** in the methylene bridges with stoichiometric amounts of hydroxide anions, forming the neutral product **48**. Subsequently the base assisted reductive elimination of HCl forms **44**. By adding equimolar hydrochloric acid the equilibrium between **40**, **48** and **44** can also *be shifted* back to **40**. From Scheme 23 it is obvious that the Ir(I) complex **44** is around 21 kcal/mol higher in energy compared to the Ir(III) species **48**. This is quite similar to the Ir(I) complexes **46** and **45** relative to their Ir(III) compounds **47** and **56**. The difference is that **44** is 16 kcal/mol and 24 kcal/mol destabilized compared to the Ir(III) complexes **56** and **47**, respectively. This is due to the increased ring strain in the five-membered ring containing the double bond.

5. Conclusion

Tridentate twofold symmetric pincer ligands as species which mold the properties and reactivity of metal atom oxidation states have matured as a growing field since their beginnings in the early 1970s. Differences between aryl, alkyl and cycloheptatrienyl backbones in the complexes with late transition metals are reflected in the diversity of their metal complex reactivity. The observation of β-elimination reactions in alkyl pincer complexes points to a high flexibility of the alkyl backbone. As a consequence of the non-activated and non-acidic C–H bonds in the alkyl backbone as well as due to a weak chloride ligand the PCP carbene complex **9** can be isolated. In contrast the chemistry of the cycloheptatrienyl PCP-pincer complexes is dominated by the acidic methylene protons and the possibility to form an aromatic tropylium cation. The planarity of the cycloheptatriene ring in **49** induces increased mobility of the methylene bridges and therefore γ-H-eliminations to the metal are observed. This and CO instead of chloride *trans* to the ring carbon are facts explaining that the carbene structure **49** is not isolated yet. From a thermodynamic point of view the β-elimination in alkyl pincer complexes and backbone rearrangements in neutral cycloheptatrienyl pincer complexes are driven by the formation of a sp^2-carbon-metal σ-bond. Although in phenyl PCP-pincer complexes the flexibility of the backbone is comparable to that of the planar cycloheptatrienyl compounds there is no driving force for backbone rearrangements like in alkyl and cycloheptatrienyl systems. Carbene structures comparable to the alkyl com-

pound **9** are only accessible in functionalized aryl PCP-pincer complexes.

Acknowledgements

We thank those students, colleagues and the funding agencies DAAD, DFG, Fond der Chemischen Industrie, National Science Foundation, Petroleum Research Fund, Studienstiftung des Deutschen Volkes, who have supported this research.

References

[1] B.L. Shaw, J. Am. Chem. Soc. 97 (1975) 3856.
[2] B.L. Shaw, J. Organomet. Chem. 200 (1980) 307.
[3] D. Morales-Morales, C.M. Jensen (Eds.), The Chemistry of Pincer Compounds, Elsevier, Amsterdam, 2007.
[4] M. Albrecht, G. van Koten, Angew. Chem. Int. Ed. 40 (2001) 3750.
[5] M.E. van der Boom, D. Milstein, Chem. Rev. 103 (2003) 1759.
[6] M. Ohff, A. Ohff, M.E. van der Boom, D. Milstein, J. Am. Chem. Soc. 119 (1997) 11687.
[7] K. Krogh-Jespersen, M. Czerw, M. Kanzelberger, A.S. Goldman, J. Chem. Inf. Comput. Sci. 41 (2001) 56.
[8] M.W. Haenel, S. Oevers, K. Angermund, W.C. Kaska, H.-J. Fan, M.B. Hall, Angew. Chem. Int. Ed. 40 (2001) 3569.
[9] C.S. Creaser, W.C. Kaska, Inorg. Chim. Acta 30 (1978) L325.
[10] C.J. Moulton, B.L. Shaw, J. Chem. Soc., Dalton Trans. (1976) 1020.
[11] P.G. Eller, D.C. Bradley, M.B. Hursthouse, D.W. Meek, Coord. Chem. Rev. 24 (1977) 1.
[12] G. van Koten, Pure Appl. Chem. 61 (1989) 1681.
[13] M. Gozin, A. Weisman, Y. Ben-David, D. Milstein, Nature 364 (1993) 699.
[14] A. Vigalok, D. Milstein, Acc. Chem. Res. 34 (2001) 798.
[15] L.C. Liang, Coord. Chem. Rev. 250 (2006) 1152.
[16] T.B. Gunnoe, Eur. J. Inorg. Chem. (2007) 1185.
[17] J.W.J. Knapen, A.W. van der Made, J.C. de Wilde, P.W.N.M. van Leeuwen, P. Wijkens, D.M. Grove, G. Van Koten, Nature 372 (1994) 659.
[18] C.M. Jensen, Chem. Commun. (1999) 2443.
[19] S. Nemeh, R.J. Flesher, K. Gierling, C. Maichle-Mössmer, H.A. Mayer, W.C. Kaska, Organometallics 17 (1998) 2003.
[20] A.M. Winter, K. Eichele, H.G. Mack, W.C. Kaska, H.A. Mayer, Organometallics 24 (2005) 1837.
[21] A.M. Winter, K. Eichele, H.-G. Mack, W.C. Kaska, H.A. Mayer, Dalton Trans. (2008) 527.
[22] N. Ashkenazi, A. Vigalok, S. Parthiban, Y. Ben-David, L.J.W. Shimon, J.M.L. Martin, D. Milstein, J. Am. Chem. Soc. 122 (2000) 8797.
[23] H.A.Y. Mohammad, J.C. Grimm, K. Eichele, H.G. Mack, B. Speiser, F. Novak, M.G. Quintanilla, W.C. Kaska, H.A. Mayer, Organometallics 21 (2002) 5775.
[24] J.C. Grimm, PhD Thesis, Universität Tübingen, 2001.
[25] J.F. Riehl, Y. Jean, O. Eisenstein, M. Pelissier, Organometallics 11 (1992) 729.
[26] K. Krogh-Jespersen, M. Czerw, K.M. Zhu, B. Singh, M. Kanzelberger, N. Darji, P.D. Achord, K.B. Renkema, A.S. Goldman, J. Am. Chem. Soc. 124 (2002) 10797.
[27] F. Novak, B. Speiser, H.A.Y. Mohammad, H.A. Mayer, Electrochim. Acta 49 (2004) 3841.
[28] A. Ceccanti, P. Diversi, G. Ingrosso, F. Laschi, A. Lucherini, S. Magagna, P. Zanello, J. Organomet. Chem. 526 (1996) 251.
[29] P. Diversi, S. Iacoponi, G. Ingrosso, F. Laschi, A. Lucherini, G. Pinzino, G. Uccello-Barretta, P. Zanello, Organometallics 14 (1995) 3275.
[30] P. Diversi, S. Iacoponi, G. Ingrosso, F. Laschi, A. Lucherini, P. Zanello, J. Chem. Soc., Dalton Trans. (1993) 351.
[31] S. Nemeh, C. Jensen, E. Binamira-Soriaga, W.C. Kaska, Organometallics 2 (1983) 1442.
[32] D. Conner, K.N. Jayaprakash, T.R. Cundari, T.B. Gunnoe, Organometallics 23 (2004) 2724.
[33] C. Crocker, H.D. Empsall, R.J. Errington, E.M. Hyde, W.S. McDonald, R. Markham, M.C. Norton, B.L. Shaw, B. Weeks, J. Chem. Soc., Dalton Trans. (1982) 1217.
[34] R.J. Flesher, PhD Thesis, University of California Santa Barbara, 1999.
[35] A. Vigalok, Y. Ben-David, D. Milstein, Organometallics 15 (1996) 1839.
[36] A. Vigalok, D. Milstein, Organometallics 19 (2000) 2061.
[37] D.G. Gusev, A.J. Lough, Organometallics 21 (2002) 5091.
[38] D.G. Gusev, A.J. Lough, Organometallics 21 (2002) 2601.
[39] V.F. Kuznetsov, K. Abdur-Rashid, A.J. Lough, D.G. Gusev, J. Am. Chem. Soc. 128 (2006) 14388.
[40] W. Weng, S. Parkin, O.V. Ozerov, Organometallics 25 (2006) 5345.
[41] J. Zhao, A.S. Goldman, J.F. Hartwig, Science 307 (2005) 1080.
[42] M. Kanzelberger, X.W. Zhang, T.J. Emge, A.S. Goldman, J. Zhao, C. Incarvito, J.F. Hartwig, J. Am. Chem. Soc. 125 (2003) 13644.
[43] M.A. McLoughlin, N.L. Keder, W.T.A. Harrison, R.J. Flesher, H.A. Mayer, W.C. Kaska, Inorg. Chem. 38 (1999) 3223.
[44] W.C. Kaska, S. Nemeh, A. Shirazi, S. Potuznik, Organometallics 7 (1988) 13.
[45] K.W. Huang, J.H. Han, C.B. Musgrave, E. Fujita, Organometallics 26 (2007) 508.
[46] M.L.H. Green, D.K.P. Ng, Chem. Rev. 95 (1995) 439.
[47] I.D. Gridnev, M.K.C. del Rosario, Organometallics 24 (2005) 4519.
[48] Z. Lu, W.M. Jones, W.R. Winchester, Organometallics 12 (1993) 1344.
[49] M. Tamm, A. Grzegorzewski, I. Brudgam, H. Hartl, J. Chem. Soc., Dalton Trans. (1998) 3523.
[50] M. Tamm, A. Grzegorzewski, I. Brudgam, H. Hartl, Chem. Commun. (1997) 2227.
[51] R.P. Johnson, Chem. Rev. 89 (1989) 1111.
[52] S. Matzinger, T. Bally, E.V. Patterson, R.J. McMahon, J. Am. Chem. Soc. 118 (1996) 1535.
[53] N.T. Allison, Y. Kawada, W.M. Jones, J. Am. Chem. Soc. 100 (1978) 5224.
[54] A.M. Winter, Diploma Thesis, Universität Tübingen, 2001.
[55] A.A. Koridze, A.M. Sheloumov, S.A. Kuklin, V.Y. Lagunova, I.I. Petukhova, P.V. Petrovskii, Russ. Chem. Bull. 52 (2003) 516.
[56] E.J. Farrington, E.M. Viviente, B.S. Williams, G. van Koten, J.M. Brown, Chem. Commun. (2002) 308.
[57] A.A. Koridze, A.M. Sheloumov, S.A. Kuklin, V.Y. Lagunova, I.I. Petukhova, F.M. Dolgushin, M.G. Ezernitskaya, P.V. Petrovskii, A.A. Macharashvili, R.V. Chedia, Russ. Chem. Bull. 51 (2002) 1077.
[58] A.A. Koridze, S.A. Kuklin, A.M. Sheloumov, F.M. Dolgushin, V.Y. Lagunova, I.I. Petukhova, M.G. Ezernitskaya, A.S. Peregudov, P.V. Petrovskii, E.V. Vorontsov, M. Baya, R. Poli, Organometallics 23 (2004) 4585.
[59] D.L. DuBois, D.M. Blake, A. Miedaner, C.J. Curtis, M.R. Dubois, J.A. Franz, J.C. Linehan, Organometallics 25 (2006) 4414.
[60] A.M. Winter, PhD Thesis, Universität Tübingen, 2004.